

Dielectrics Newsletter

Scientific newsletter for dielectric spectroscopy

Issue July 1994

Prof. J.H.Wendorff, Th.Fuhrmann

Dielectric spectroscopy and the interaction of light and matter

*May not bodies receive much of their activity
from the particles of light
which enter into their composition ?
Isaac Newton, Opticks*

The investigation of light-induced phenomena in matter is one of the most interesting research topics in the interdisciplinary field between physics, chemistry and material science. Both structure and dynamics may be influenced by light, giving rise to important technological applications of various photochromic materials. In this contribution we focus on the application of liquid crystalline side chain polymers in optical data storage. Here, dielectric spectroscopy serves as a tool for investigating the molecular relaxations involved in the storage mechanism. We present an experimental setup for dielectric measurement during irradiation of the sample and show first results.

Light-induced reorientation in LCP's containing azo chromophores

The possibility of using liquid crystalline polymers (LCP) for reversible optical data storage was first demonstrated in 1987 [1], using copolymers with azo chromophoric mesogens like the compound shown in figure 1.

The underlying storage principle is

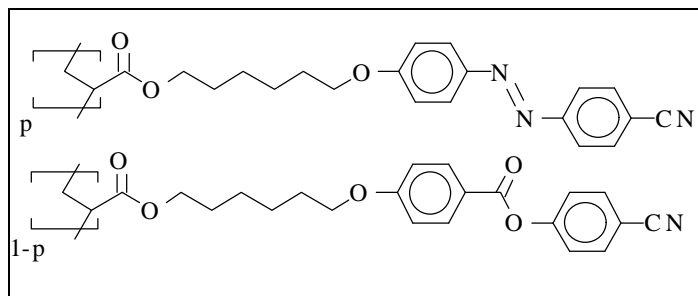


Fig. 1 : compound

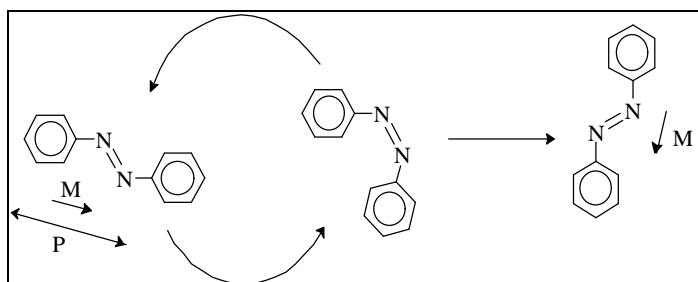


Fig. 2: Photoisomerization cycle

as follows: When irradiated with polarized light at an appropriate wavelength, the azo dye molecules attached to the polymer backbone undergo photoinduced trans-cis-trans isomerization cycles (figure 2).

In each isomerization step they are able to change their orientation in the matrix. Considering the fact that the excitation probability depends on the orientation of the transition moment (M) relative to the polarization plane (P) of the light, the mesogenic side chains tend to orient finally perpendicular to that plane (figure 3), because in that orientation they can no longer take part in the isomerization cycles.

The macroscopic effect is therefore a realignment of the optical axis, accompanied by a modulation of the index of refraction at the illuminated spots. This modulation can be used for storing holographic or digital

information.

It is obvious that the rotational motion of the mesogenic groups around the backbone determines the dynamics of the storage process, and this is, in terms of dielectric spectroscopy, the δ -relaxation of LCP's. Of course, light induced and electric field induced rotations are not directly comparable, because they take place on different time scales and follow different mechanisms. Nevertheless, dielectric measurements can provide important information about the motion of the mesogenic side chains in the matrix such as activation energies and so on.

The question is to what extent the matrix will be influenced by the

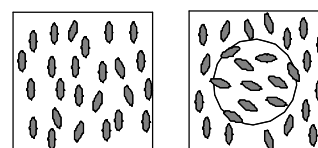


Fig.3: Photoinduced Reorientation

photochemical isomerization process. The isomerizing molecules are expected to increase the local free volume, making the reorientation of the side chains easier. Indeed, holographic measurements show evidence for a permanent effect on the matrix structure: once free volume has been introduced, the orientation evidently becomes faster. Another remarkable effect is the decrease of the phase transition temperature T_{NI} due to local

(NOVOCONTROL) by constructing a special sample holder which allows direct measurement during irradiation of the sample (figure 4)

Hardware adaptation: Dielectric measurement during irradiation

Light is introduced into the sample holder using a light wave guide which is linked with an argon ion laser operating at 488 nm. The capacitor containing the sample

Temperature control is obtained by NOVOCONTROL's QUATRO. All measurements were performed in the temperature range from 0°C to 100°C and in a frequency range from 20 Hz up to 10 kHz, limited by the DC resistance of the ITO coating.

Measurements

We examined various fractions of the copolymer mentioned above, consisting of 6-(4-(4-cyanophenylazo)-phenoxy)-hexyl-acrylate and 6-(4-(4-cyanophenoxy-carbonyl)-phenoxy)-hexyl-acrylate in different ratios (0 to 80% azo monomer content).

Previous studies on oriented samples [2] revealed that there are two relaxations in the temperature domain between 0°C and 120°C (figure 5). The first one exhibits a negative dielectric anisotropy $\Delta\epsilon = \epsilon_{//} - \epsilon_{\perp}$, and there are contributions to $\tan\delta$ in both directions. The WLF-like temperature dependence and the coupling to the "static" glass transition, defines this as α -relaxation. The second one is characterized by a strongly positive dielectric anisotropy, the relaxation maximum being visible only in $\tan\delta_{//}$. It is a single relaxation, giving a semicircular Cole-Cole-plot (ϵ'' vs. ϵ') and shows an Arrhenius-like temperature dependence. Being assigned to the reorientation of the long axis of the mesogenic groups (δ -relaxation), this is the relaxation on which we will focus now.

The modification of the relaxation under irradiation is shown in figure 6 for the copolymer with $p=40\%$. Here, $\tan\delta$ is plotted vs. frequency for different temperatures. Measurements without light (upper diagram) and measurements under irradiation with 70 mW/cm² at 488 nm (lower diagram) are directly compared. As expected, we see that the δ -relaxation is remarkably shifted to higher frequencies. The reorientation of the mesogens becomes faster, and this means that the isomerization process of the azo chromophores will provide local free volume for the side chain

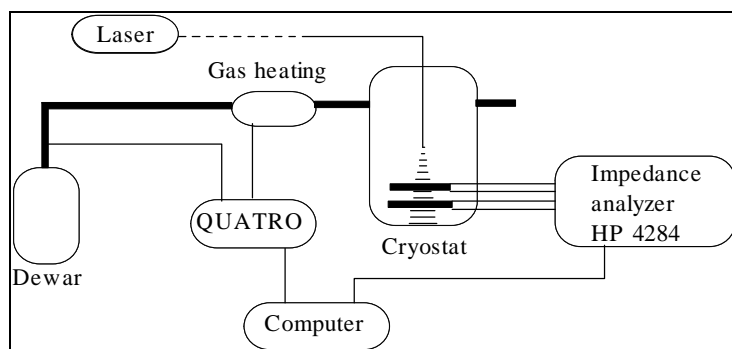


Fig. 4 : Experimental setup

perturbations of the liquid crystalline order caused by the isomerization process. The magnitude of this effect is reported to be up to 20°C.

consists of two crossed sheets of glass coated with indium-tin-oxide (ITO), so that both conductivity and transparency are guaranteed. Samples

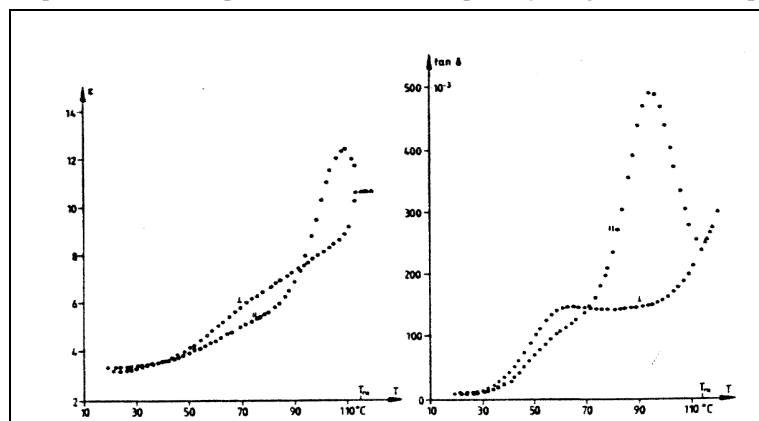


Fig. 5: Dielectric anisotropy for the copolymer with $p=30\%$, measured at 10 kHz

Dielectric spectroscopy as an independent method may help to characterize the influences of irradiation on molecular relaxation processes.

For our purposes it was necessary to measure the dielectric properties in the presence of light. Therefore, we modified a standard setup for dielectric measurements

are prepared directly from the melt without macroscopic alignment and annealed overnight in the liquid crystalline phase.

The sample capacitor is connected with an impedance analyzer (HP 4248 A) using the four-terminal pair configuration. Connections between capacitor and electric circuit are made with conducting glue.

movement.

Accordingly, a closer look to the temperature dependence of the relaxation maxima shows a shift of the line in the Arrhenius plot (figure 7). The activation energy calculated from the slope decreases by a small amount but not significantly. Thus, the influence of irradiation on the

collected in table 1. It contains T_g and T_{NI} , measured by DSC (Differential Scanning Calorimetry), the activation energies obtained without and under irradiation, and the frequency acceleration factor f at 80°C.

The latter is defined as the ratio of the relaxation frequencies with and

large deviation, because they are dependent on the thermal history of the sample. The expected error due to thermal heating was estimated to be in the order of 0.1°C.

An important question concerns the distribution of the relaxation times, i.e. whether it is modified or not. To answer this question a Havriliak-Negami-Fit was made. We followed the method according to Kremer et al. /3/ which takes also the DC conductivity into account:

$$\epsilon''(\omega) = \epsilon_\infty + \frac{\epsilon - \epsilon_\infty}{(1 + (i\omega\tau_0)^{-\alpha})^\beta} + i \frac{d_0}{\omega^{1-s}}$$

p	Tg	TNI	DHact	DHact (irrad.)	f
0	37.5°C	118.2°C	182 kJ/mol	173 kJ/mol	1.06
20 %	39.5°C	120.5°C	190 kJ/mol	178 kJ/mol	2.0
40 %	40.7°C	122.1°C	167 kJ/mol	163 kJ/mol	2.9
60 %	39.3°C	123.8°C	151 kJ/mol	143 kJ/mol	1.7
80 %	39.9°C	130.6°C	149 kJ/mol	140 kJ/mol	2.6

Table 1

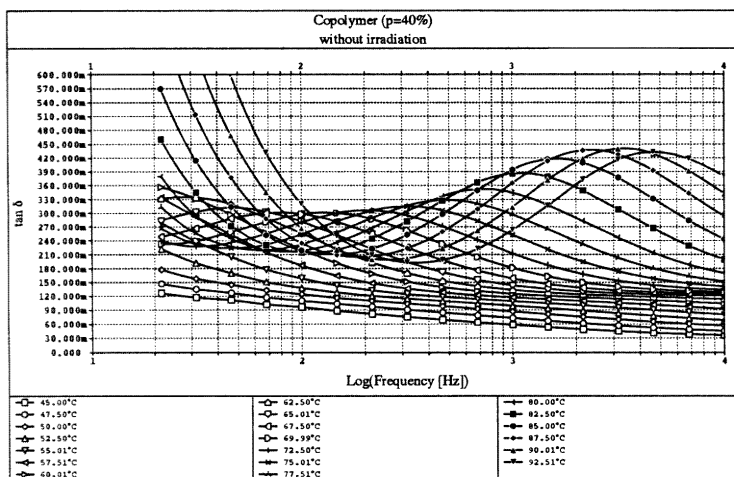
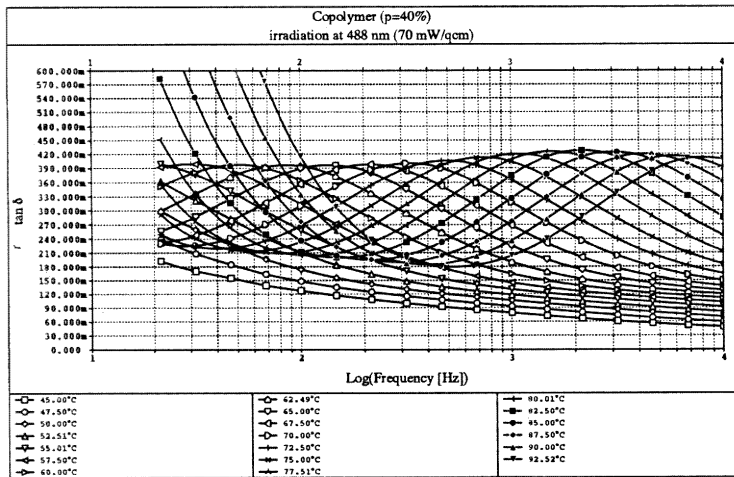


Fig.6 a,b: d-relaxation without and with irradiation

activation energies is almost negligible. The data for different fractions of the copolymer are

without irradiation.

The absolute values of the frequency shift may have a relatively

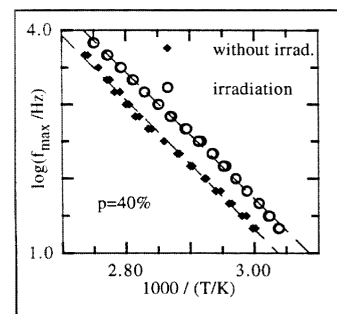


Fig. 7: Arrhenius plot

The values obtained for α and β lie in the range of 0.1 to 0.2 and 0.6 to 0.9, respectively, indicating a small relaxation time distribution. It is shown as $G(\ln\tau)$ in figure 8. In addition to the acceleration of the relaxation we see a slight broadening in the relaxation time distribution.

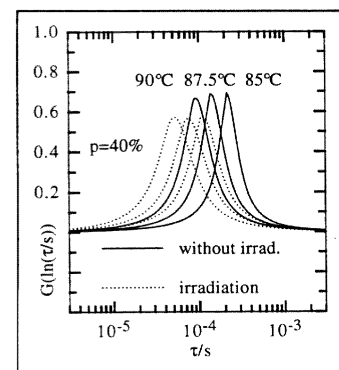


Fig. 8: Relaxation time distribution

In summary, we were able to detect characteristic effects of irradiation on the dielectric relaxation behaviour of LCP's containing azo chromophores. The δ -relaxation which describes the rotation of the mesogenic side chains is accelerated by light. The effect is

relatively small, but nevertheless detectable and must be taken into account in the discussion of light induced reorientation phenomena in photochromic LCP's. This will help us to get a better insight into the fundamental processes involved in optical storage.

References

- /1/ M.Eich, J.H.Wendorff, B.Reck, H.Ringsdorf, Makromol. Chem., Rapid Commun. **8**, 59 (1987)
 /2/ R.Birenheide, M.Eich, B.W.Endres, H.Hirschmann, O.Schönherr, J.H. Wendorff, 17. Freiburger Arbeitstagung Flüssigkristalle, März 1987
 /3/ F.Kremer, S.U.Vallerien, R.Zentel, H.Kapitza, Macromolecules **22**, 4040 (1989)

Prof. Joachim H. Wendorff
 Thomas Fuhrmann
 FB Physikalische Chemie
 Philipps-Universität Marburg
 Hans-Meerwein-Straße
 35032 Marburg
 Germany

F. Kremer

Collective and molecular dynamics in liquid crystals

Dielectric spectroscopy in its modern form is a versatile tool for the study of the molecular dynamics of polymers and liquid crystals: It is broadband in frequency covering the range from 10^{-4} Hz up to 10^{10} Hz or higher, thus making possible the study of both fast processes (e.g.

within a polymer its dynamics can be studied. For liquid crystalline side group polymers, for instance, five different relaxation processes were found.^[1] For combined main chain side group systems the systematic chemical variation of the dipoles revealed three relaxation processes.^[2] These are schematically shown in Figure 1.

The α -relaxation corresponds to the dynamic glass transition the β_m -relaxation is assigned to the hindered rotation (libration) of the main-chain

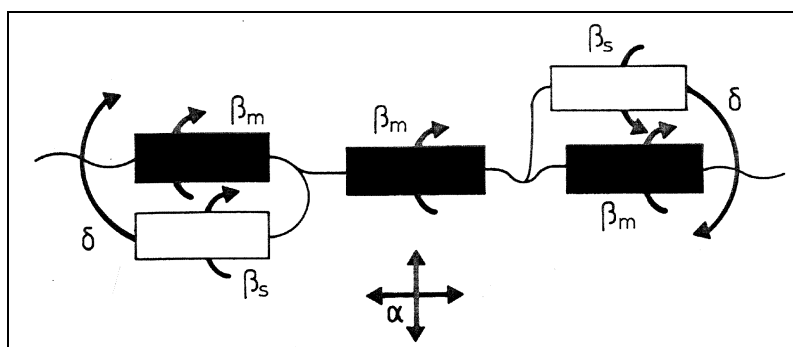


Fig.1: Scheme of the movements inside the liquid crystalline polymers assigned to the observed relaxation processes

rotation of a mesogenic group around its long molecular axis) and slow relaxations (e.g. the α -relaxation close to the calorimetric glass transition). With optimized sample preparation techniques the amount of sample material required can be reduced to less than 10 mg. The

mesogen around its long molecular axis, and the β_s -relaxation is assigned to the libration of the side group mesogen around its long molecular axis.

For side group polymers, a collective relaxation process (δ -process) was found^[1,3-7] which is

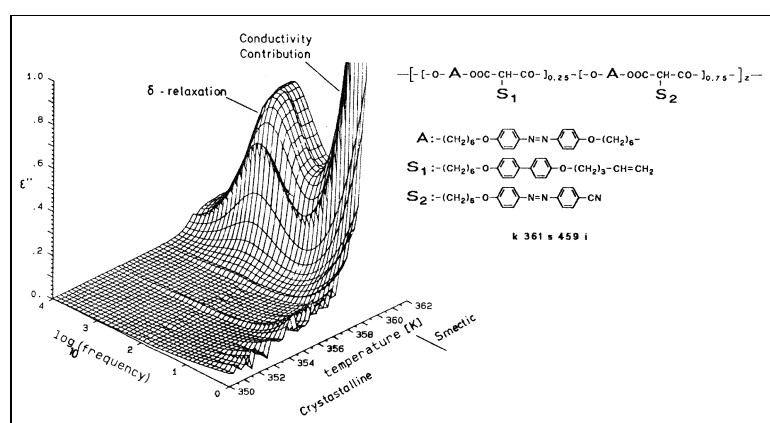


Fig.2: Dielectric loss ϵ'' vs. temperature and frequency at the transition smectic/crystalline.

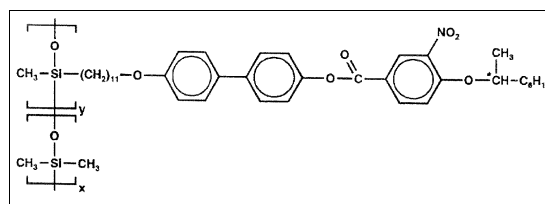
sensors made use of in the determination of the molecular dynamics are molecular dipoles. If these dipoles are placed systematically in different positions

assigned to the hindered rotation of the side groups around the polymeric main chain. The cooperativity of this process was analyzed by adding low molar mass systems to the liquid

crystalline side chain polymer.^[8] A similar process was found for a combined main chain side group liquid crystalline polymer.^[9] For a related copolymer^[10] the suppression of this δ -relaxation at the smectic/-crystalline phase transition was observed (Fig.2).

Since liquid crystalline compounds were found to have ferroelectric properties in chiral tilted smectic phases (for example S_C^* - phase)^[11], there have been many affords to understand and optimize their ferroelectric behavior (high saturation polarization, short switching times etc.). Besides a lot of synthetical work^[12] and structure investigations^[12] the molecular and collective dynamics of low molecular weight ferroelectric liquid crystals (FLC) has been investigated by several techniques as NMR^[13], light scattering^[14], dielectric spectroscopy^[15-17] and is well understood. In 1984 the first ferroelectric liquid crystalline polymers were synthesized^[18]. These materials combine the properties of low molecular weight FLC with the typical properties of polymers. Further on the liquid crystalline phases were stabilized by the polymer main chain which leads to much broader mesophases than in the analogous low molecular weight compounds. The combination of both the ferroelectric and the polymeric properties leads to new applications, for example as flexible displays. For such applications the dynamical behaviour has also to be understood.

In the frequency regime from 10^{-2} to 10^9 Hz three dielectric loss processes can be observed (Fig.3a/b). Two of them (Goldstone - and soft - mode) occur at frequencies below 1MHz. Their huge dielectric losses indicate their collective character. In the frequency regime above 1MHz one dielectric relaxation is found. Its comparably low dielectric loss underlines the local character of this relaxation process, which is not restricted to the liquid crystalline phase.



$$x : y = 3.2 : 1 \quad 90 S_X \quad 46 S_C^* \quad 98 S_A \quad 144 i.s.$$

Fig. 3a: Chemical structure and phase sequence of the ferroelectric copolymer

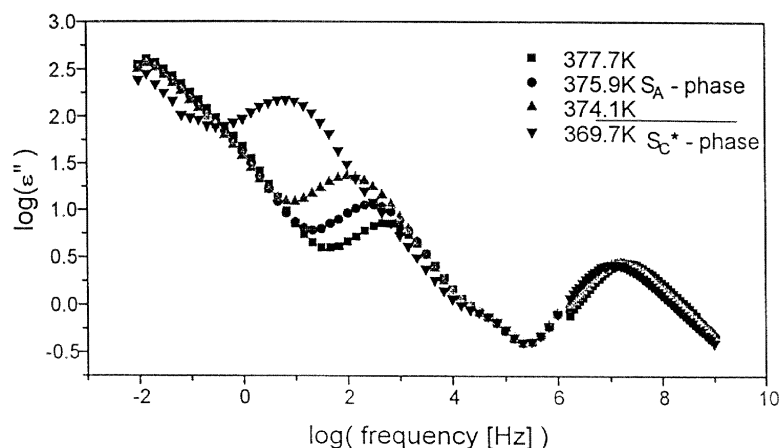


Fig.3b: $\log(\epsilon'')$ vs. $\log(\text{frequency})$ measured over 11 decades for a ferroelectric copolymer. The experimental error is estimated to be not larger than the size of symbols.

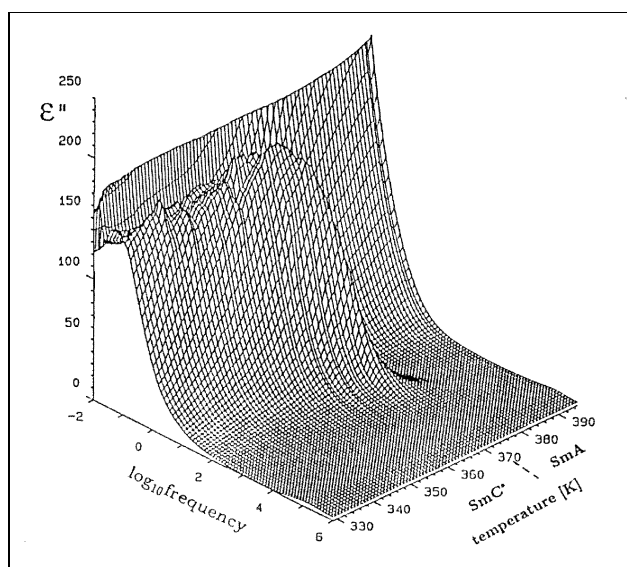


Fig.4: The Goldstone - mode in a ferroelectric copolymer

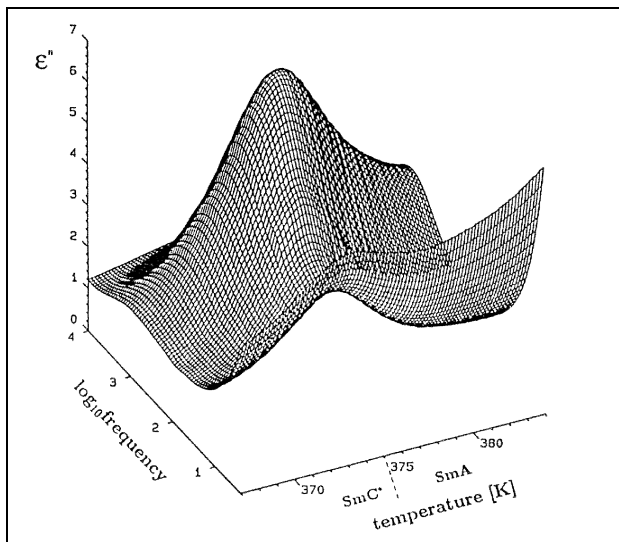


Fig.5: The soft - mode in a polymeric FLC (sample: ferroelectric copolymers),
 $E = 15 \text{ kV/cm}$, sample thickness: $10 \mu\text{m}$

Collective dynamics of ferroelectric polymers

In the frequency range below 1MHz the dielectric spectrum is dominated by one very huge relaxation (Goldstone - mode), which is restricted to the S_{C^*} - phase (Fig.4). It is assigned to the fluctuation of the phase of the helical superstructure. Comparing this process with the Goldstone - mode in the analogous low molar mass compound the relaxation is shifted

usually is only weakly temperature dependent. Superimposing a DC - bias field unwinds the helical superstructure. By this the Goldstone - mode can be suppressed continuously. In the unwound state a second loss process (soft - mode) becomes observable again. In order to study the soft - mode behaviour in more detail the measurements were repeated with a superimposed DC - bias field (Fig.5).

The soft - mode, which is assigned to the fluctuation of the tilt, increases

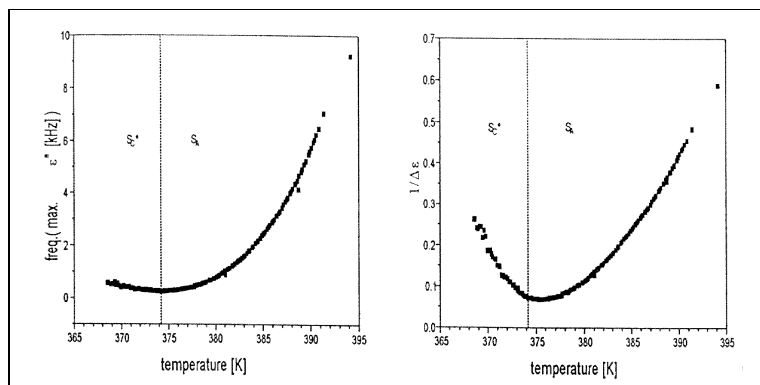


Fig.6: a) Frequency of the max. ϵ'' vs. temperature
 b) inverse dielectric strength vs. temperature
 (sample: ferroelectric copolymer)
 $E = 15 \text{ kV/cm}$, sample thickness: $10 \mu\text{m}$.

nearly two decades to lower frequencies. Additionally the Goldstone - mode shows a pronounced temperature dependence while in low molar mass FLC's this

in the S_A - phase, has a maximum at the phase transition S_A/S_{C^*} and decreases in the S_{C^*} - phase. As the phase transition S_A/S_{C^*} is of second order the following theoretical

predictions for the soft - mode dynamics near this transition have to be fulfilled: (i) The frequency position of the maximum dielectric loss should obey a Curie Weiss law, (ii) for this temperature dependence the slope in the S_{C^*} - phase should be twice as much as in the S_A - phase, (iii) for the inverse of the dielectric strength a similar Curie - Weiss temperature dependence is predicted.

For the further analysis the experimental data were fitted by use of the generalized relaxation function according to Havriliak and Negami. The inverse of the dielectric strength shows a comparable temperature dependence (Fig.6) as predicted and as it is found for low molar mass FLC's.

The frequency of the maximum ϵ'' only corresponds in the S_A - phase. Although the soft - mode should increase in its frequency position in the S_{C^*} - phase, it remains at nearly the same frequency position. This may be due to viscosity effects from the polymer main chain or from an insufficient suppression of the Goldstone - mode. Additionally the phase transition occurs not as sharp as for low molar mass compounds, but this is a general feature of polymeric FLC's.

Molecular dynamics of FLC - polymers

In the frequency regime above 1MHz one dielectric loss process - the β - relaxation - can be observed (Fig.7).

It is assigned to be hindered rotation (libration) of the mesogene around its long molecular axis and has a comparable low intensity as expected for a local process. The measured loss curves can be well described with the Havriliak - Negami equation. The relaxation time shows no discontinuities at the phase transition S_A/S_{C^*} , especially there is no slowing down observable. By cooling down from the isotropic phase and by entering the S_{C^*} - phase, the dielectric strength $\Delta\epsilon$ increases, because due to the formation of the bookshelf geometry

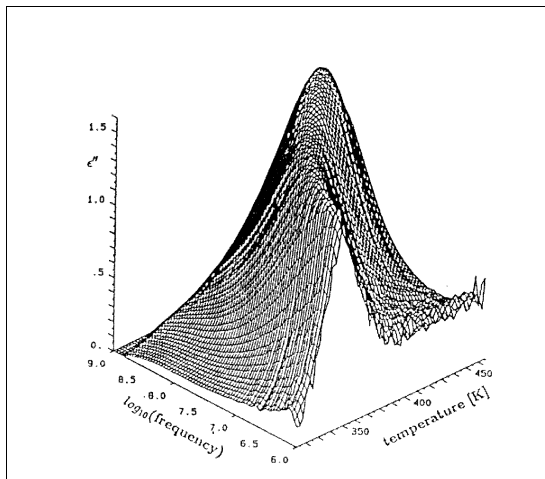


Fig.7: The β -relaxation in a ferroelectric copolymer, sample thickness: 20 μm .

the aspect angle of the dipole moment interacting with the outer electric field changes. By the same argument there is a small step at the phase transition S_A/S_C^* . As the alignment in the high frequency measurements is only partially achieved, these steps are not as pronounced as for low molar mass systems.

In summary broadband dielectric spectroscopy reveals as a very versatile tool to study the collective and molecular dynamics of liquid crystals.

References

- [1] R.Zentel, G.R.Strobl, H.Ringsdorf, *Macromolecules* 18 (1985) 960
- [2] F.Kremer, S.U.Vallerien, R.Zentel, H.Kapitza, *Macromolecules* 22 (1989) 4040
- [3] H.Kresse, S.Kostromin, V.P.Shibaev, *Makromol.Chem.Rapid Commun.* 3 (1982) 509
- [4] S.U.Vallerien, F.Kremer, C.Boeffel, *Liq.Cryst.*4 (1989) 79
- [5] B.Stoll, W.Heinrich, *Colloid Polym.Sci.* 263 (1985) 895
- [6] G.S.Attard, G.Williams, G.W.Gray, D.Lacey, P.A.Gemmel, *Polymer* 27 (1986) 185
- [7] W.Haase, F.Pranoto, F.J.Bormuth, *Ber.Bunsenges.Phys.Chem.* 89 (1985) 1229
- [8] H.Seiberle, W.Stille, G.R.Strobl, *Macromolecules* 23 (1990) 2008
- [9] B.W.Endress, J.H.Wendorff, B.Reck, H.Ringsdorf, *Makromol.Chem.* 188 (1987) 1501
- [10] S.U.Vallerien, Diploma-Thesis, University of Mainz 1988
- [11] R.B.Meyer, L.Liebert, L.Strzlecki, P.J.Keller, *J.Phys.(Paris) Lett.*36 (1975) L69
- [12] G.B.McArdle, "Side Chain Liquid Crystal Polymers", Blackie Publishing Group, Glasgow 1989
- [13] A.Yoshizawa, H.Kikuzaki, T.Hirai, M.Yamane, *Jpn.J.Appl.Phys.* 28 (1989), 1988
- [14] J.Musevic, R.Blinic, B.Zeks, C.Filipic, M.Copic, A.Seppen, P.Wyder, A.M.Levanyuk; *Phys.Rev.Lett.* 60 (1988), 1530
- [15] F.Gouda, G.Andersson, S.T.Lagerwall, K.Skarp, B.Stebler, T.Carlsson, B.Zeks, C.Filipic, A.Levstik; *Liq.Cryst.* 6, (1989) 219
- [16] A.M.Biradar, S.Wrobel, W.Haase, *Phys. Rev. A* 39 (1989), 2693
- [17] A.Schönfeld, F.Kremer, R.Zentel, *Liq.Cryst.* 13 (1993), 403
- [18] F.Kremer, A.Schönfeld, R.Zentel, H.Pothes, *Polym.Adv.Techn.* 3 (1992), 249

[18] V.P.Shibaev, M.Z.Kozlovsky, L.A.Beresnev, L.M.Blinov, N.A.Plata, *Polymer Bull.* 12(1984), 299

Prof. Dr. F. Kremer
Universität Leipzig, Institut für Physik,
Linnéstr. 5, 04103 Leipzig, Germany

Dr. Gerhard Schaumburg

New broadband dielectric spectrometers

A series of new broadband dielectric spectrometers are available now by NOVOCONTROL. All systems are based on frequency

Introduction

response analysis and are combinations of the new NOVOCONTROL Broadband Dielectric Converter BDC with either the new STANFORD Lock-In Amplifiers SR 850, SR 830 or SR 810 or the Impedance/ Gain-Phase Analyzers SI 1260 or SI 1255.

The BDC is a new development from NOVOCONTROL which has been optimized for highest precision in $\tan(\delta)$ accuracy over a broad frequency range. New features are the variable reference standard which is matched automatically to the sample impedance, an active sample cell and an additional passive measurement procedure at high frequencies. Moreover, the BDC is designed to work in combination with both gain-phase analyzers and lock-in amplifiers.

The digital lock-in amplifiers SR 850, SR 830 or SR 810 are offered by STANFORD RESEARCH SYSTEMS for about one year. In contrast to conventional analog lock-in amplifiers, digital phase sensitive detectors are used allowing to operate the lock-in technique also at low frequencies. The main advantage of the lock-in-amplifiers is their price being below a quarter of an impedance/gain-phase analyzer.

Principle of measurement

The principle of measurement is shown in fig. 1.

The sample material with the complex dielectric function $\epsilon(f)$ is placed between the plates of a sample capacitor. The ac voltage U with the frequency of measurement f is applied to the sample capacitor by the generator. The resistor R converts the sample current I into a voltage. The

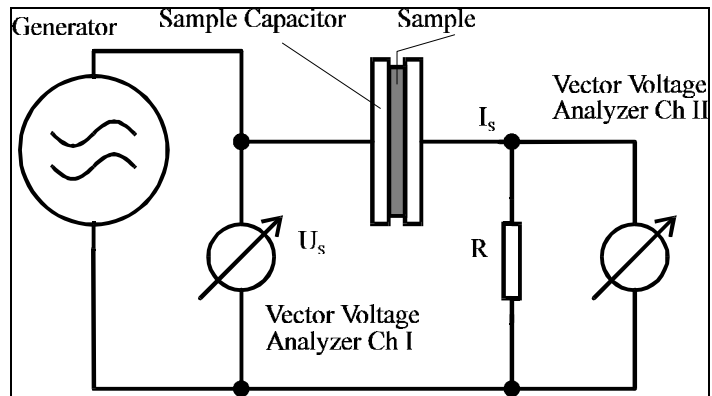


Fig. 1: Principle of a dielectric measurement using frequency response analysis

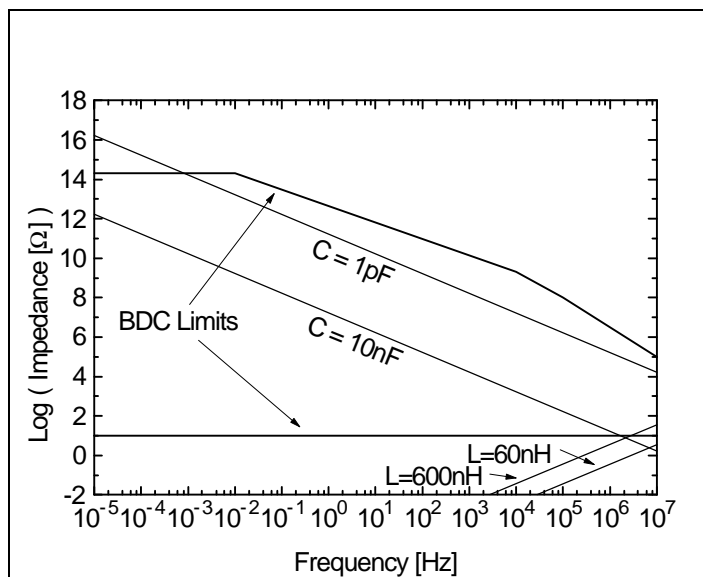


Fig. 2: Impedance of two low loss sample capacities, of 1m BNC cable (600nH) and of the air insulated lines of the BDC active sample cell (60nH).

amplitudes and the phases of U and the sample current I are measured by two phase sensitive voltage meters. If

$$Z = U/I \quad (1)$$

denotes the impedance of the sample capacitor, its complex capacity is calculated from

$$C = \frac{-i}{2\pi f Z} \quad (2).$$

Neglecting border effects, the dielectric function is obtained from the standard equation of a parallel capacitor

$$\epsilon = \epsilon' - i\epsilon'' = \frac{Cd}{\epsilon_0 A} \quad (3)$$

where d is the distance between the plates, A the area of one plate and ϵ_0

the vacuum permittivity.

The frequency response measurement has to be compared with the competition technique of time domain. In a time domain measurement, the sample capacitor is excited by a voltage step instead by an ac signal. Afterwards the voltage is kept constant and the decay of the sample current is measured as a function of time. The dielectric function is calculated by a discrete Fourier transformation of the time dependent current. The features of the both techniques are shown in tab. 1.

Although the frequency response technique is a direct and simple method, in practice some problems arise. As can be seen from (2) the impedance of a low loss sample

increases with decreasing frequency. The impedance of typical sample capacities in the frequency range from 10^{-5} - 10^7 Hz is shown in fig. 2 and covers a range of 16 orders of magnitude. Moreover, for low loss - or conductive samples, the phase angle has to be measured with extraordinary high precision. A further problem arises at frequencies above 100 kHz. In this range, the serial impedance caused by the inductivity of the measurement lines contributes as additional error to the sample impedance.

NOVOCONTROL Broadband Dielectric Converter BDC

It is the purpose of the BDC to overcome these difficulties. The BDC replaces the resistor R in fig. 1 by a more sophisticated current to voltage converter. Moreover it allows to compare each sample impedance point with a build in variable reference capacity which improves accuracy in phase resolution. The principle of measurement for low frequencies below 100 kHz is shown in fig. 3.

Z_X is a variable impedance which can be changed in resistance and capacity. The sample impedance Z_S of a direct measurement (no reference) is given by

$$Z_S = \frac{U_{1S}}{I_S} = - \frac{U_{1S}}{U_{2S}} Z_X \quad (4)$$

Reference measurement

Although (4) is valid for ideal components, it leads to results with are accurate only in the percent range, due to phase errors in current to voltage converter and the analyzer. This accuracy is improved if a reference measurement under the same conditions is taken. Z_X is then calculated by

$$Z_X = \frac{U_{2R}}{I_R} = - \frac{U_{2R}}{U_{1R}} Z_C \quad (5)$$

where Z_C is the impedance of the reference capacitor (see (2)). With the combination of (4) and (5), the sample impedance becomes independent of Z_X

	Frequency Domain	Time Domain
Measured quantity	Direct phase sensitive measurement of sample voltage $U(f)$ and current $I(f)$ at fixed frequency	Measurement of the time dependent decay current $I(t)$ of the sample capacitor which was excited by a voltage step U_S
Evaluation of data	Simple : $Z(f) = \frac{U(f)}{I(f)}$	Complex : $Z(\omega) = - \frac{iU_S}{\omega} \frac{1}{\int_0^{\infty} I(t) e^{-i\omega t} dt}$ $(\omega=2\pi f)$
Accuracy	High	Medium
Measurement time	About $1/f + 1/f$ settling time for each frequency point, about $3/f_{min} + 3/f_{min}$ settling time for an entire spectrum with 7 points/decade	About $1/f_{min} + 1/f_{min}$ settling time for the entire spectrum
Impedance range	Very large, as measurement gain can be selected for each frequency	Limited, as measurement gain generally can not be changed during the sweep
Measurement technique	Lock-in technique, which suppresses all frequency components except f	Direct sampling of $I(t)$ with an analog digital converter
Noise sensitivity	Low, as noise is suppressed by lock-in technique	High, as noise enters directly to the measured signal
Leakage current sensitivity	Low, as suppressed by ac-filter	High, as leakage current can not be separated from $I(t)$
$U(f)$ or U_S drift sensitivity	Low, as suppressed by ac-filter	High, as drifts in U_S enter directly into $I(t)$
Verification of results	Easy, as measured data are direct linked with results	Difficult, as measured data are linked with results by numerical Fourier transformation

Table 1 : Comparison between the principles of frequency domain - and time domain measurements.

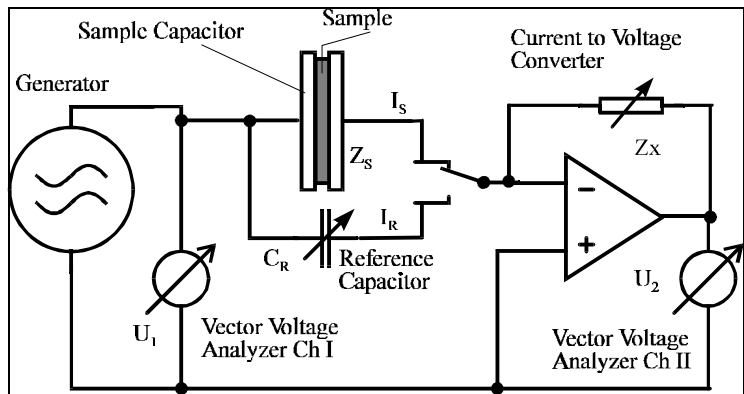


Fig. 3 : BDC principle at frequencies > 100 kHz.

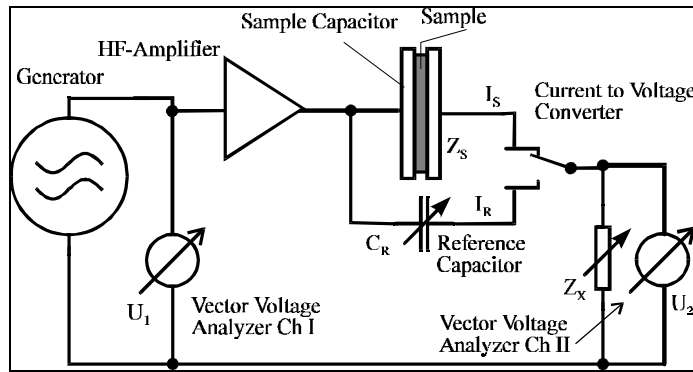


Fig. 4 : BDC principle at high frequencies > 100 kHz.

$$Z_S = \frac{U_{1S}}{I_S} = -\frac{U_{1S}}{U_{2S}} \frac{U_{2R}}{U_{1R}} Z_C \quad (6)$$

As the Z_x calculated from (5) contains all linear deviations of the entire system, these linear errors are eliminated by the reference technique.

Nevertheless, some sources of systematic errors as non linear distortions in the BDC and the analyzer remain active. These effects can be neglected, if the difference between sample and reference impedance is kept small enough. In this case, the analyzer measures nearly identical values for the sample and the reference measurement and the measurement is only limited by the analyzer resolution (the accuracy for reproducing values at constant input voltage). In practise, non linear errors occur if the sample impedance differs more than 10 % from the reference impedance. Therefore, the BDC reference impedance can be adjusted in 64 steps between 25 pF and 2 nF. In the auto reference mode, the BDC selects automatically the reference capacity which matches to the sample.

High frequency set-up

In the low frequency set-up (fig. 3), an operational amplifier is used being able to handle extreme low input currents down to 40 fA and therefore the performance for high impedance measurements is excellent. On the other hand these amplifiers are limited to frequencies below

approximately 100 kHz.

Therefore, the BDC uses at high frequencies another principle of current to voltage conversion, which is drawn in fig. 4.

The ac voltage of the analyzer generator drives the HF-buffer amplifier, which decouples the sample current from the analyzer. In contrast to fig. 4, the active current to voltage converter is replaced by a passive variable impedance Z_x . For ideal components and neglected line effects, Z_S is calculated from

$$Z_S = Z_X \frac{1 - m_S}{m_S} \quad (7)$$

with

$$m_S = \frac{U_{2S}}{U_{1S}} \quad (8).$$

The reference technique can be applied in the same manner as described above.

Active sample cell version

The BDC is available in two versions. The first is the BNC-version, where the sample is placed into a separate sample cell which is connected by BNC cables to the BDC. Although this arrangement is very flexible, the excellent high frequency performance of the BDC is limited by inductivities of the BNC lines which are in series with the sample capacity. This effect is reduced in the BDC active sample cell version shown in fig 5.

Here the complete analog electronics is mounted on top of the

sample cell and the connection lines to the sample capacitor is done with solid air insulated lines having only a tenth of the inductivity of 1 meter BNC cable as shown in fig 2. The active sample cell fits directly into the NOVOCONTROL standard cryostats and can be used at temperatures from -200°C to +400°C.

Lock-in amplifiers

One of the most interesting new features of the BDC is, that it can also be used with vector voltage analyzers having only one channel (instead of two for measuring U_2 and U_1) without losing accuracy or increasing measurement time. This is achieved by additional internal

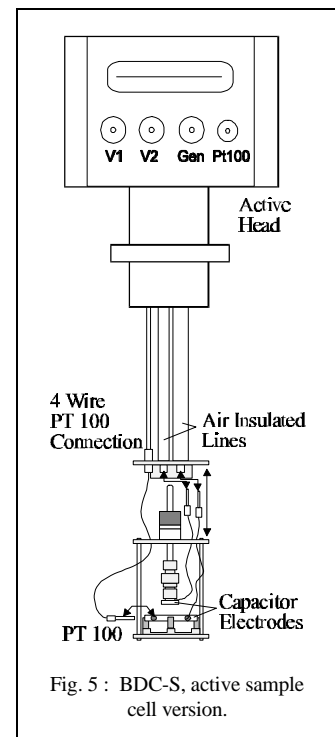


Fig. 5 : BDC-S, active sample cell version.

electronics, allowing to access the complex voltage ratio of U_2 and U_1 at a single port of the BDC. Therefore lock-in amplifiers which are known to be high precision devices can be used as vector analyzers for the BDC. The lock-in amplifiers STANFORD SR 850, SR 830 and SR 810 are supported as standard analyzers by NOVOCONTROL dielectric measurement systems. They are a series of new digital lock-in amplifiers with 16 bit analog digital

converters and operate from 1 mHz to 100 kHz. In combination with the BDC, a resolution in $\tan(\delta)$ better than 10^{-4} over the entire frequency range is achieved (10^{-3} above 30 kHz). The impedance range is 10 Ω to $2 \cdot 10^{14}$ Ω . The main advantage of the lock-in is, that its price is much lower than a two channel gain/phase analyzer. This enables NOVOCONTROL to offer complete dielectric measurement systems including BDC, lock-in amplifier, PC, WinDETA software, sample cell, and temperature control below \$60.000. These systems can be seen as an economical high quality solution for scientific applications, which do not need the frequency range above 100 kHz. This systems are also ideally suited for the quality assurance (QA) of polymers, resins, colloids, etc. in industry. They are in the same price class as solutions based on impedance bridges but are much more accurate and moreover the NOVOCONTROL system covers the low frequency range below 30 Hz, in which the bridge techniques generally fail (see previous Dielectrics Newsletter, Overview : Modern measurement techniques in Broadband Dielectric Spectroscopy).

Impedance/gain phase analyzers

These are the analyzers SI 1260 or SI 1255. They can be used in combination with the BDC between 10^{-5} Hz and 10^7 Hz. This combination can be seen as a high end system which is setting the pace in dielectric instrumentation. Like the systems with lock-in amplifiers, it covers the impedance range from 10 Ω to $2 \cdot 10^{14}$ Ω with $\tan(\delta) < 10^{-4}$. The main difference to the lock-in amplifiers is the extended frequency range and the two independent measurement channels of the analyzers. In addition, the SI 1260 has a third current channel, allowing to measure impedance from 10 m Ω to 100 M Ω with resolution in $\tan(\delta) < 0.3$ %. Thus the whole system covers an impedance range of 16 decades. If a proper sample geometry is selected,

specific conductivity from 10^5 S/cm to 10^{-18} S/cm can be measured.

Measurement control and software

All measurement systems operate fully automated under control of a PC with the MS-WINDOWS (TM) software package WinDETA. WinDETA supports the independent variables frequency, temperature,

time and dc-bias. These four variables can be arranged in arbitrary order, and therefore define a measurement arrangement up to four dimensions. The results are graphically displayed in 2- or 3-dimensional diagrams. Diagrams are printed with high resolution on any printer supported by MS-WINDOWS (TM) and can be exported into other programs. Data are saved either as

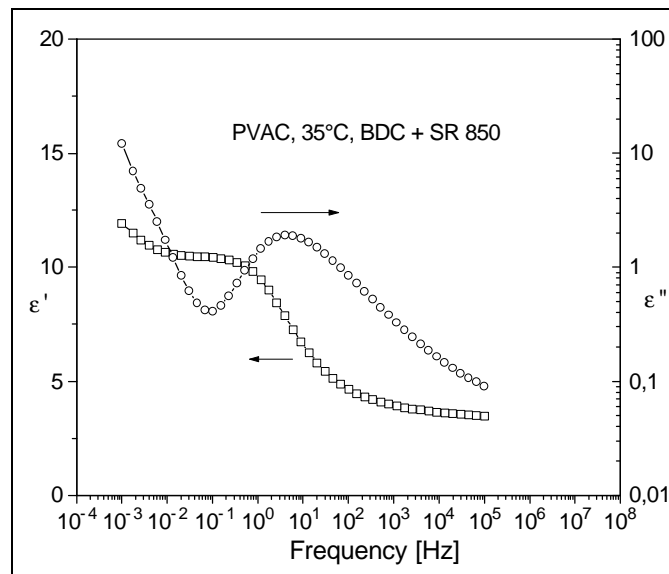


Fig. 7: Example measurement of PVAC at 35° C with the devices Novocontrol BDC and SR 850.

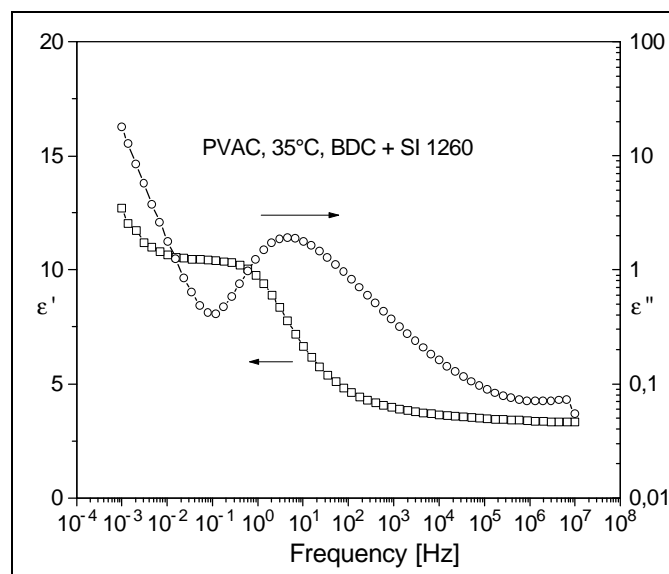


Fig. 6 : Example measurement of PVAC at 35° C with the devices Novocontrol BDC and SI 1260.

ASCII tables or binary files in various formats. WinDETA includes control of the devices (NOVOCONTROL BDC, SI 1260, SI 1255, STANFORD SR 850, SR 830, SR 810, HEWLETT PACKARD HP 4191 and HP 4284), calibration of the measurement lines and devices, control of the measurement procedure and evaluation of the impedance data.

Measurement examples

In fig. 6 and fig. 7 example measurements of Polyvinylacetat (15000 g/mol) are shown. They were done at a temperature of 35 °C and show the performance of the Novocontrol BDC in combination with either the Stanford SR 850 lock-in amplifier or the SI 1260 frequency response analyzer. Both

measurements show the α -relaxation in the middle frequency range and a conductivity contribution at low frequencies.

Dr. Gerhard Schaumburg,
NOVOCONTROL GmbH,
Obererbacher Str. 9, 56414 Hundsangen,
Germany

Dielectrics Newsletter is published by:

Novocontrol GmbH
Obererbacher Str. 9
56414 Hundsangen
Germany
☎ ++49 - 6435 - 96230
fax: ++49 - 6435 - 962333

Editors:

Dr. Gerhard Schaumburg
Robert den Dulk

Abstracts and suggestions are always welcome. Send these directly to the publisher.

YES

send me the following issues of the Dielectrics Newsletter.
I will receive the 1994 issues free.

NOVOCONTROL GmbH
- Dielectrics Newsletter -
Obererbacher Str. 9

56414 Hundsangen
Germany

name: _____
company or _____
University _____
adress: _____
